On the thermodynamic approach towards time-series analysis



1994 J. Phys. A: Math. Gen. 27 3029

(http://iopscience.iop.org/0305-4470/27/9/018)

J. Phys. A: Math. Gen. 27 (1994) 3029–3049. Printed in the UK

# On the thermodynamic approach towards time-series analysis

Wolfram Just

Theoretische Festkörperphysik, Technische Hochschule Darmstadt, Hochschulstraße 8, D-64289 Darmstadt, Germany

*Received 10 June 1993, in final form 20 December 1993*

**Abstract.** A scheme is presented which allows for the computation of the topological pressure and power spectra associated with equilibrium measures from a given time series. Its convergence properties are demonstrated on numerical data sets obtained from the Lozi and the Henon map. Numerical evidence for sharp peaks in the power spectrum of the non-hyperbolic phase is given and supported by estimates using periodic-orbit expansions.

## 1. Introduction

Chaos in nonlinear dynamical systems is a well known phenomenon nowadays. On a phenomenological level it is quite well understood and has been observed experimentally in a lot of systems. In sharp contrast to the detailed study of theoretical models there are only a few different approaches to analysing time series directly. The properties of chaotic motion favour the application of statistical methods which have the aim of studying the structure of the physical invariant distribution (SRB measure in mathematical terms). One type of method deals with fractal aspects of the invariant distribution and uses generalized dimensions and singularity spectra for a quantitative description (e.g. [1–9] for experimental results). As these quantities contain information about the metric structure of the system this approach demands a phase-space reconstruction technique which is a field of intense research in its own right (e.g. [10] and references therein). A different type of method deals with the correlation properties which are beyond the usual double time correlation analysis. They are the subject of interest for this paper. There seems to be no general relationship between these two kinds of approaches. However, they yield the same information under special mathematical preconditions.

From the theoretical point of view the investigation of local time averages and their statistical properties have been proven to be useful [11–17] even in some experimental contexts [18]. The approach is widely equivalent to a thermostatic formulation of spin systems† and a lot of concepts have been carried over from ordinary statistical mechanics [19–21]. The basic quantity of interest is given by the local average of some (observed) quantity $u_t$. It contains important information about the local structure of the dynamics. To be consistent with the notation in the literature the time series is assumed to be generated by some discrete dynamical system $x_{n+1} = T(x_n)$ and some phase-space observable $u(x)$. But this assumption is not important for the subsequent discussions. The fluctuations of the

† If a generating partition is available, the corresponding symbolic dynamics allows for an explicit construction of the spin system.

0305-4470/94/093029+21$19.50  

local average $U_n(x) = \sum_{k=0}^{n-1} u(T^k(x))/n$ are most conveniently studied via the characteristic function

$$\Phi(q) = \lim_{n\to\infty} \frac{1}{n} \ln\langle \exp(qnU_n(x))\rangle \tag{1}$$

also termed the topological pressure in the mathematical literature. $\langle\cdots\rangle$ denotes an average with respect to the (physical) invariant distribution which is assumed to be equivalent to a long-time average with respect to a typical time series

$$\langle g(x)\rangle = \lim_{N\to\infty} \frac{1}{N} \sum_{k=0}^{N-1} g(T^k(x)) . \tag{2}$$

The parameter $q$ plays the important role of singling out the local structures. This can be easily understood by inspecting the derivative of the characteristic function, which reads

$$\langle u\rangle(q) = \frac{\mathrm{d}\Phi}{\mathrm{d}q} = \lim_{n\to\infty} \frac{\langle U_n(x)\exp(qnU_n(x))\rangle}{\langle \exp(qnU_n(x))\rangle} = \int u(x)\,\mathrm{d}\mu_q . \tag{3}$$

The last equality states the well known fact [20, 22] that the limit can be written† as an average with respect to an invariant measure $\mu_q$, usually called an equilibrium measure in the mathematical literature. Although this measure is in general not accessible, the expectation value (3) can be computed via a long-time average of the kind (2) which contains an additional exponential weight factor. Different invariant measures that mean different subsets of the attractor are singled out depending on the observable $u(x)$ and the parameter $q$. They can be investigated by the average (3). Properties which are related to phase-space regions that are rarely visited by typical trajectories can be studied in a systematic way. In this sense, the local properties of the system can be investigated.

The quantities (1) and (3) only contain some averaged information about the local properties. Even this is an important feature, as singular local structures show up in phase transitions [17, 23–27]. Qualitatively different kinds of the dynamics can be detected by this approach. Nevertheless, a more detailed analysis is desirable. For this reason the investigation of time correlations via correlation functions and power spectra is meaningful [28]:

$$\begin{aligned} C_q(k) &= \lim_{n\to\infty} \frac{1}{n} \sum_{j=0}^{n-1} \langle u(T^{j+k}(x))u(T^j(x))\exp(qnU_n(x))\rangle / \langle \exp(qnU_n(x))\rangle \\ &= \int u(T^k(x))u(x)\,\mathrm{d}\mu_q \\ I_q(\omega) &= \lim_{n\to\infty} \frac{1}{n} \left\langle \left| \sum_{k=0}^{n-1} u(T^k(x))\mathrm{e}^{-\mathrm{i}\omega k} \right|^2 \exp(qnU_n(x)) \right\rangle \Big/ \langle \exp(qnU_n(x))\rangle \\ &= \lim_{n\to\infty} \frac{1}{n} \int \left| \sum_{k=0}^{n-1} u(T^k(x))\,\mathrm{e}^{-\mathrm{i}\omega k} \right|^2 \mathrm{d}\mu_q . \end{aligned} \tag{4}$$

From the theoretical point of view the quantities (1) and (4) have proven to be a useful tool in understanding the dynamics of nonlinear chaotic systems on a detailed level [29–33]. It is obvious that they reduce to ordinary statistical averages (SRB averages) in the case $q = 0$, because the exponential weight factor vanishes. This property reflects the fact that the corresponding equilibrium measure $\mu_{q=0}$ reduces to the Sinai–Ruelle–Bowen measure. Ordinary averages usually contain many different statistical aspects of the system under consideration, e.g. the structure of periodic orbits and non-hyperbolic points determine the shape of the

† On a mathematically rigorous level the relation is proven for hyperbolic or expanding systems.

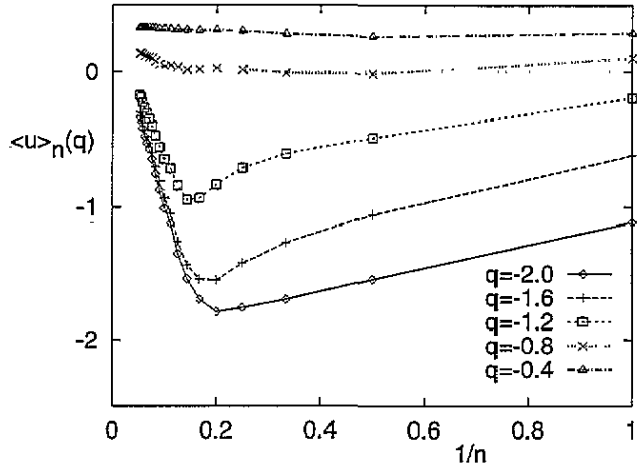


**Figure 1.** Dependence of the derivative of the topological pressure on the local-time coarse graining $n$ for the Henon map ($a = 1.4$, $b = 0.3$) obtained from a finite ensemble of size $N = 3 \times 10^7$. The local expansion rate is chosen as observable $u(x)$.

power spectra in a complicated way [34]. One possibility to shed some light on the intricate structure of the invariant distribution without making a phase-space reconstruction or having knowledge of the actual dynamical equations is the investigation of the $q$-dependence of the thermodynamic quantities (1) and (4). In particular, singular local structures which violate the uniform hyperbolicity in chaotic systems, e.g. tangency points of local stable and unstable manifolds in dissipative systems or cantori in Hamiltonian dynamics, show up with non-analytic behaviour which are usually called phase transitions.

An application of (1), (3) and (4) to (experimental) time series seems to be straightforward. But the finite size $N$ of the available ensemble poses some constraint on the length $n$ of the local-time coarse graining. If the latter quantity is chosen to be too large, the exponential weight factor in expressions like (3) approaches, for almost all initial conditions, the asymptotic form $\exp(qn\langle u\rangle)$ and cancels in the numerator and denominator. Hence, the quantity $\langle u\rangle(q)$ tends towards the ordinary long-time average $\langle u\rangle(q = 0)$. As an example, figure 1 shows the $n$-dependence of the average (3) obtained from a numerically generated time series of length $N = 3 \times 10^7$ of the Henon map. If $n$ is chosen considerably larger than $\sim 10$, the convergency towards the ordinary long-time average is clearly observed. This tendency reflects the fact that an ensemble of size $N$ cannot capture the important correlations of the local averages $U_n(x)$ if the time coarse graining is chosen too large. With the help of a generating partition of the dynamical system an estimate like $N \gtrsim e^{cn}$ can be derived to ensure that the limits $N \to \infty$ and $n \to \infty$ are obtained in the correct way.

On the other hand, the computation of correlation functions and power spectra (4) requires large $n$ values, especially if the long-time, low-frequency behaviour has to be resolved. Furthermore, spectra obtained from low $n$ values are rather noisy if no ensemble average is performed (cf figures 3 and 5).

These two competitive effects cause some problems and may yield misleading results if the thermodynamic quantities (1) and (4) are calculated directly [35, 36]. Methods are required to infer the limit from the low-$n$ behaviour. Such a method has been introduced on a formal level in terms of a continued-fraction expansion for the quantity (1) [37, 38]. But its practical convergence behaviour has not been discussed except for model systems. On

the other hand, it has been observed that spurious solutions in such a kind of expansion may arise [39, 40]. I want to analyse these methods from the point of view of their convergence properties. Section 2 reviews the approach, explains the origin of the spurious solutions, and gives simple prescriptions for their treatment. The scheme is tested on some time series obtained from numerical solutions of simple maps and the convergence behaviour is demonstrated. Similar ideas are then developed and tested for the computation of the power spectrum (4) from the short-time behaviour of the correlation function. As a by-product, some results on the time correlations in the non-hyperbolic phase of the Henon map are obtained. Finally, the results which have been computed via numerical simulations are checked from a theoretical viewpoint by a periodic-orbit expansion. This approach sheds some more light on the interpretation of the thermodynamic quantities (4).

## 2. Continued-fraction expansion for the topological pressure

Although the continued-fraction expansion for the quantity (1) is well known [37, 38] its properties are not discussed in the literature. To keep the presentation self-contained let me review briefly the main ideas of the expansion. The characteristic function is determined by the exponential growth rate of the averages

$$M_n(q) = \langle \exp(qnU_n(x)) \rangle . \tag{5}$$

It is the goal of the following considerations to extract this rate from the behaviour at low $n$ values. The quantities (5) are related to the moments of the transfer operator [41, 42]

$$(\mathcal{H}_q^u h)(x) = \int \delta(x - T(y))\, \mathrm{e}^{qu(y)} h(y)\, \mathrm{d}y \tag{6}$$

via

$$M_n(q) = \int ((\mathcal{H}_q^u)^n \rho_*)(x)\, \mathrm{d}x . \tag{7}$$

Here $\rho_*$ denotes the invariant density. Obviously the logarithm of the largest eigenvalue $\lambda_q^{(0)}$ of the operator (6) yields the characteristic function (1), whereas the remaining part of the spectrum determines the correlation function and the power spectrum (4) [28]. To evaluate the eigenvalues of the transfer operator a projection-operator technique can be applied to its resolvent (cf appendix A). This approach leads to the matrix element

$$R(z) = \left( \frac{1}{z\mathbf{1} - \omega\chi^{-1} - \Gamma(z)} \chi \right)_{11} . \tag{8}$$

The eigenvalues are determined by the poles of this expression. The $M \times M$ matrices $\chi$ and $\omega$ are given by

$$\chi = \begin{pmatrix} M_0(q) & \dots & M_{M-1}(q) \\ \vdots & & \vdots \\ M_{M-1}(q) & \dots & M_{2M-2}(q) \end{pmatrix} \qquad \omega = \begin{pmatrix} M_1(q) & \dots & M_M(q) \\ \vdots & & \vdots \\ M_M(q) & \dots & M_{2M-1}(q) \end{pmatrix} \tag{9}$$

and the index in (8) denotes the upper-left matrix element. The memory matrix $\Gamma(z)$ has only one non-vanishing element in the lower-right corner and is of no interest in the subsequent discussion. It should be mentioned that this matrix element vanishes if the transfer operator admits an $M$-dimensional invariant subspace which contains the invariant density (cf appendix A). This condition holds especially for the case of piecewise linear one-dimensional maps [43]. Expression (8) can be cast into the form of a continued fraction expansion of order $M$ if the memory matrix is neglected. Its coefficients are given by

algebraic expressions in the moments (5) and can be computed from a time series without making any reference to transfer operators. In fact, the continued-fraction expansion can be derived formally without recourse to transfer operators [37]. In view of the previous remark the expansion can be interpreted as an approximation of the full dynamical system by a piecewise linear one which is a special case of an approximation by Markov models.

We are interested in the poles of the continued fraction of order $M$ which yield an approximation for the pressure. They are determined by the algebraic equation

$$0 = \det(\chi z - \omega) = \det\omega \cdot (-\det) \begin{pmatrix} z & M_2(q) - M_1(q)M_1(q) & \dots & M_M(q) - M_1(q)M_{M-1}(q) \\ z^2 & M_3(q) - M_2(q)M_1(q) & \dots & M_{M+1}(q) - M_2(q)M_{M-1}(q) \\ \vdots & \vdots & & \vdots \\ z^M & M_{M-1}(q) - M_M(q)M_1(q) & \dots & M_{2M-1}(q) - M_M(q)M_{M-1}(q) \end{pmatrix}. \tag{10}$$

Equation (10) can be cast into the form of a polynomial

$$\sum_{k=0}^{M} c_k z^k = 0. \tag{11}$$

In view of the special structure of the second determinant in (10) the coefficients $c_k$ obey the following set of linear equations:

$$\sum_{k=0}^{M} M_{n+k}(q)c_k = 0 \qquad 0 \leqslant n \leqslant M-1. \tag{12}$$

They determine the coefficients up to some unimportant common factor. As long as the matrix $\chi$ is invertible, relation (10) is equivalent to (11) and (12). They define a set of equations to determine the pressure.

However, there arises a problem due to spurious poles of the continued fraction expansion. They are related to the fact that the matrices (9) may become non-invertible if the order $M$ of the expansion is increased. Hence, these solutions are not related to the convergence behaviour of the continued fraction, which is well understood [44] but to a singular behaviour of its coefficients. To make this statement explicit let us for the moment consider a system whose transfer operator admits the above-mentioned invariant subspace of order $M_0$, e.g. a piecewise linear one-dimensional map. On this subspace the operator obeys its characteristic equation, which is in fact a polynomial of degree $M_0$

$$\sum_{k=0}^{M_0} d_k (\mathcal{H}_q^u)^k = 0. \tag{13}$$

Owing to (7) we obtain exact linear relations between the moments (5)

$$\sum_{k=0}^{M_0} d_k M_{k+n}(q) = 0 \tag{14}$$

which cause the matrices (9) to become non-invertible in the case $M > M_0$. As a consequence, the general solution of (12) reads

$$(c_0, \dots, c_M) = \alpha_0(d_0, \dots, d_{M_0}, 0, \dots, 0) + \alpha_1(0, d_0, \dots, d_{M_0}, 0, \dots, 0) + \cdots + \alpha_{M-M_0}(0, \dots, 0, d_0, \dots, d_{M_0}) \tag{15}$$

by taking the relations (14) into account. The coefficients $\alpha_k$ are as yet undetermined. The polynomial (11) which determines the pressure results in

$$0 = \sum_{k=0}^{M_0} d_k z^k \sum_{k=0}^{M-M_0} \alpha_k z^k . \tag{16}$$

The first factor yields the exact eigenvalues whereas the second term is as yet undetermined.

If (14) holds exactly the continued fraction expansion (10) terminates at order $M = M_0$ and generates the exact eigenvalues. But even for piecewise linear dynamical systems the numerically generated moments $M_n^{\text{num}}(q)$ will contain small numerical and statistical errors $\delta M_n(q)$ which denote the deviation from the unknown exact value $M_n(q) = M_n^{\text{num}}(q) - \delta M_n(q)$. They prevent (14) from being valid. As a consequence, the matrices (9) are invertible in the generic case and (12) admits a solution $c_k^{\text{num}}$ which is unique up to a common factor. Inspecting the result (15) the coefficients $c_k^{\text{num}}$ read

$$\begin{aligned}(c_0^{\text{num}}, \ldots, c_M^{\text{num}}) = \alpha_0^{\text{num}}(d_0, \ldots, d_{M_0}, 0, \ldots, 0) + \alpha_1^{\text{num}}(0, d_0, \ldots, d_{M_0}, 0, \ldots, 0) + \cdots \\ + \alpha_{M-M_0}^{\text{num}}(0, \ldots, 0, d_0, \ldots, d_{M_0}) + (\delta c_0, \ldots, \delta c_M)\end{aligned} \tag{17}$$

where the contributions $\delta c_k$ are of the order of the statistical and numerical errors. The coefficients $\alpha_k^{\text{num}}$ have finite values and are determined by the perturbations $\delta M_n(q)$ in a complicated way. We end up with the result (16) if we neglect the terms of order $\delta M_n(q)$. The second factor yields spurious poles.

The arguments given above, for piecewise linear maps, can also be applied to a general dynamical system. In this case, an invariant subspace which has the above-mentioned properties is not likely to exist. Hence (14) ceases to be valid. But the moments (7) are mainly determined by the eigenvalues with large absolute values. Therefore they depend mainly upon the leading, say $M_0$, eigenvalues up to some small contribution $\delta M_n(q)$. The reasoning of the preceding paragraph can be applied to this situation. Again spurious solutions emerge due to statistical and numerical errors for large orders of the expansion.

Having clarified the origin of the spurious solutions, several strategies can be developed to detect the true ones. One approach which has been used in [40] investigates the poles by switching the parameter $q$ adiabatically. This strategy requires the evaluation of (11) and (12) for a large set of $q$ values. A different and more direct approach uses the fact that the spurious solutions depend sensitively on small perturbations which are added to the moments. Equations (11) and (12) are evaluated several times using moments which contain a small additive random number. The true solutions are fixed by the requirement that they vary in a smooth way. This criterion works well in all the computations that have been performed.

To test the above-mentioned algorithm numerical calculations on discrete dynamical systems $x_{n+1} = T(x_n)$ have been performed. From a time series of length $N$ the moments have been computed and the characteristic function evaluated. Special attention has been paid to the frequently used hyperbolic Lozi map and the non-hyperbolic Henon map

$$\begin{aligned} x_{n+1}^{(1)} &= 1 - a|x_n^{(1)}| + bx_n^{(2)} & \qquad x_{n+1}^{(1)} &= 1 - a\left(x_n^{(1)}\right)^2 + bx_n^{(2)} \\ x_{n+1}^{(2)} &= x_n^{(1)} & \qquad x_{n+1}^{(2)} &= x_n^{(1)} . \end{aligned} \tag{18}$$

The local expansion rate $\lambda(x)$ is chosen as the observable $u(x)$ because it is of special importance for the structure of the invariant distribution and is frequently discussed in the literature [19, 25, 45, 46]. As far as the simulations show, the applicability of the algorithm does not depend on this special choice. $\lambda(x)$ determines the rate of local expansion of nearby phase-space points. It can easily be computed by applying the linearized map $DT(x)$ to unit vectors $e_k$ via $\exp(\lambda(x_n))e_{n+1} = DT(x_n)e_n$ [29]. It is worth mentioning that this quantity

**Table 1.** Topological pressure of the Lozi map at parameter values $a = 1.7$, $b = 0.5$ obtained *from a time series of length* $N = 10^5$. $\Phi_{cf}$ *denotes the continued-fraction result of order* $M$, $\Phi_{2M-1}$ the result of the direct computation by choosing $n = 2M - 1$, and $\Delta$ the determinant of the truncated matrix representation of the transfer operator. The last column contains reference values obtained for $N = 9.5 \times 10^8$ and $n = 40$.

| | | $M = 2$ | $M = 3$ | $M = 4$ | $M = 5$ | |
|---|---|---|---|---|---|---|
| $q = -3$ | $\Phi_{cf}(q)$ | $-1.1100$ | $-1.1105$ | $-1.0947$ | $-1.0941$ | $-1.1075$ |
| | $\Phi_{2M-1}(q)$ | $-1.1952$ | $-1.1620$ | $-1.1433$ | $-1.1321$ | |
| | $\Delta$ | $0.11 \times 10^{00}$ | $-0.13 \times 10^{-03}$ | $-0.27 \times 10^{-05}$ | $-0.14 \times 10^{-08}$ | |
| $q = -2$ | | $-0.7920$ | $-0.7952$ | $-0.7858$ | $-0.7855$ | $-0.7948$ |
| | | $-0.8381$ | $-0.8216$ | $-0.8125$ | $-0.8065$ | |
| | | $0.56 \times 10^{-01}$ | $-0.13 \times 10^{-03}$ | $-0.44 \times 10^{-06}$ | $-0.83 \times 10^{-10}$ | |
| $q = -1$ | | $-0.4306$ | $-0.4335$ | $-0.4299$ | $-0.4289$ | $-0.4339$ |
| | | $-0.4432$ | $-0.4392$ | $-0.4372$ | $-0.4358$ | |
| | | $0.16 \times 10^{-01}$ | $-0.19 \times 10^{-04}$ | $-0.11 \times 10^{-07}$ | $-0.78 \times 10^{-12}$ | |
| $q = 1$ | | *0.5035* | *0.4974* | *04995* | *0.5001* | *0.4998* |
| | | 0.4945 | 0.4967 | 0.4972 | 0.4978 | |
| | | $0.15 \times 10^{-01}$ | $-0.34 \times 10^{-04}$ | $-0.22 \times 10^{-07}$ | $0.24 \times 10^{-11}$ | |
| $q = 2$ | | 1.0602 | 1.0352 | 1.0452 | 1.0435 | 1.0456 |
| | | *1.0338* | *1.0392* | *1.0401* | *1.0417* | |
| | | $0.55 \times 10^{-01}$ | $-0.47 \times 10^{-03}$ | $-0.15 \times 10^{-05}$ | $-0.62 \times 10^{-09}$ | |
| $q = 3$ | | 1.6501 | 1.5908 | 1.6222 | 1.6229 | 1.6228 |
| | | 1.6070 | 1.6145 | 1.6154 | 1.6174 | |
| | | $0.11 \times 10^{00}$ | $-0.18 \times 10^{-02}$ | $-0.14 \times 10^{-04}$ | $-0.33 \times 10^{-08}$ | |

*has nothing to do with the eigenvalues of DT because the local unstable directions* $e_k$ contain correlations of the time series in a complicated way [47].

Table 1 summarizes typical results obtained for the Lozi map with parameter values $a = 1.7$, $b = 0.5$ and a moderate ensemble size of $N = 10^5$. The values of the topological pressure obtained from the continued-fraction expansion $\Phi_{cf}(q)$ are displayed for increasing order of the expansion. They are compared with the value $\Phi_{2M-1}(q) := \ln M_{2M-1}(q)/(2M-1)$ which corresponds to the highest moment that enters the expansion. Furthermore, the last column contains results which have been obtained from a huge ensemble ($N = 9.5 \times 10^8$, $n = 40$). They serve as reference values. If we estimate the size of the statistical errors roughly as $\sim N^{-1/2}$, one recognizes that the expansion converges even for small orders $M \sim 3$. However, the difference between the expansion and the direct simulation $\Phi_{2M-1}(q)$ is small except for negative $q$ values ($q = -3$) where the latter converge rather slowly. Due to the hyperbolic structure of the Lozi map, an approximation of the dynamics by a few relevant eigenvalues—that means an approximation of the transfer operator by a low-dimensional matrix—is sufficient. This causes the rapid convergence of the expansion. One can support this argument by inspecting the normalized determinant of the matrix (9) $\Delta := \exp[-(M-1)(M-2)\Phi_{2M-1}(q)]\det\chi$†. It indicates the degree of linear independence among the quantities (5) and is therefore a measure of to what extent the relation (13) or (14) is satisfied. The strong decrease of this quantity with the order of the approximation indicates that the transfer operator admits approximately a three-dimensional invariant subspace in the $q$-range investigated. Higher-order expansions induce spurious

† The normalization is necessary to compensate for the exponential dependence of the matrix elements on the row and column indices.

**Table 2.** Topological pressure of the Henon map at parameter values $a = 1.4$, $b = 0.3$ obtained from a time series of length $N = 10^5$. $\Phi_{cf}$ denotes the continued-fraction result of order $M$, $\Phi_{2M-1}$ the result of the direct computation by choosing $n = 2M - 1$, and $\Delta$ the determinant of the truncated matrix representation of the transfer operator. The last column contains reference values obtained for $N = 9.5 \times 10^8$ and $n = 25$.

| | | $M = 2$ | $M = 3$ | $M = 4$ | $M = 5$ | |
|---|---|---|---|---|---|---|
| $q = -0.2$ | $\Phi_{cf}(q)$ | −0.0781 | −0.0807 | −0.0807 | −0.0808 | −0.0806 |
| | $\Phi_{2M-1}(q)$ | −0.0789 | −0.0800 | −0.0801 | −0.0803 | |
| | $\Delta$ | $0.14 \times 10^{-02}$ | $-0.20 \times 10^{-04}$ | $-0.34 \times 10^{-08}$ | $0.35 \times 10^{-11}$ | |
| $q = -0.4$ | | −0.1420 | −0.1534 | −0.1531 | −0.1536 | −0.1527 |
| | | −0.1450 | −0.1500 | −0.1504 | −0.1514 | |
| | | $0.82 \times 10^{-02}$ | $-0.39 \times 10^{-03}$ | $-0.46 \times 10^{-06}$ | $0.23 \times 10^{-08}$ | |
| $q = -0.6$ | | −0.1857 | −0.2125 | −0.2118 | −0.2134 | −0.2119 |
| | | −0.1922 | −0.2046 | −0.2053 | −0.2087 | |
| | | $0.26 \times 10^{-01}$ | $-0.24 \times 10^{-02}$ | $-0.74 \times 10^{-05}$ | $0.13 \times 10^{-06}$ | |
| $q = -0.8$ | | −0.1991 | −0.2417 | −0.2417 | −0.2435 | −0.2509 |
| | | −0.2105 | −0.2317 | −0.2324 | −0.2418 | |
| | | $0.62 \times 10^{-01}$ | $-0.86 \times 10^{-02}$ | $-0.11 \times 10^{-04}$ | $0.16 \times 10^{-05}$ | |
| $q = -1$ | | −0.1663 | −0.2053 | −0.2053 | −0.2054 | −0.2585 |
| | | −0.1858 | −0.2022 | −0.2040 | −0.2324 | |
| | | $0.12 \times 10^{00}$ | $-0.19 \times 10^{-01}$ | $-0.41 \times 10^{-05}$ | $0.10 \times 10^{-04}$ | |
| $q = -1.2$ | | −0.0674 | −0.0852 | −0.0348 | −0.0799 | −0.2307 |
| | | −0.1035 | −0.0715 | −0.0920 | −0.1661 | |
| | | $0.21 \times 10^{00}$ | $-0.22 \times 10^{-01}$ | $-0.11 \times 10^{-01}$ | $0.25 \times 10^{-01}$ | |

solutions which are suppressed by the above-mentioned prescription.

In the presence of phase-transition points further difficulties arise because of degeneracies in the spectrum of the transfer operator. As long as the transition is caused by a small number of eigenvalues [30, 31] the continued-fraction expansion converges well. But the situation becomes more complicated for transitions in which a continuous part of the spectrum is involved. To discuss this complicated situation the Henon map has been analysed. It is well known that this system admits at standard parameter values $a = 1.4, b = 0.3$ non-hyperbolic points which produce a phase transition in the pressure at $q \simeq -1$ [46]. Table 2 summarizes typical results in the vicinity of the phase-transition point. They have been obtained from an ensemble of size $N = 10^5$. In the hyperbolic phase $q > -1$ the properties of the expansion are comparable to the Lozi map. If the phase-transition point is approached, the increase of the quantity $\Delta$ signals that an increasing number of eigenvalues enter the evaluation. This observation seems to be in accordance with the assumption that the phase transition is caused by a continuous part of the spectrum [22, 25, 26, 33]. We will dwell on this effect in the next sections. All values are compared with reference values obtained from a huge ensemble ($N = 9.5 \times 10^8$, $n = 25$). The agreement fails to be quantitative in the non-hyperbolic phase. This behaviour is not only attributed to the convergence properties of the expansion but also to the accuracy of the reference values (cf figure 1 and the remarks made in the introduction).

Summarizing the findings it has been demonstrated that the pressure can be efficiently computed via (11) and (12) even for ensembles of moderate size, that spurious solutions can be suppressed successfully, and that a quantitative measure for the convergence properties can be given. But near complicated phase-transition points the quantitative values fail to converge accurately.

### 3. Power spectra from correlation functions

The direct computation of the power spectrum (4) faces several difficulties. To perform the limit $n \to \infty$ accurately, the local-time coarse graining $n$ has to be chosen sufficiently large. As this value also determines the range of the Fourier transform, a small value causes tremendous oscillations of the spectrum (cf figure 3). Alternatively, the spectrum can be computed via the Wiener–Khinchin theorem [28]

$$I_q(\omega) = \sum_{k=-\infty}^{\infty} C_q(|k|)\, \mathrm{e}^{\mathrm{i}\omega k} \,. \tag{19}$$

To avoid a strongly oscillating power spectrum, the long-time behaviour of the correlations has to be taken into account. That means that the summation has to be truncated at sufficiently large $k$ values. But for the calculation of the corresponding correlation function (4) a constraint like $k \lesssim n$ has to be imposed. Therefore, a direct calculation of the spectrum requires sufficiently large $n$ values which, in view of the discussion of the preceding section, demands a huge ensemble size†. To overcome this difficulty, a well known continued-fraction expansion can be applied for the evaluation of the power spectrum [48,49]. To keep the presentation self-contained, its derivation in the present context is sketched in appendix A. The main idea of the expansion is quite simple. To truncate the series (19) at low order the correlation function is approximated by exponentially decaying functions. By a resummation of these expressions the oscillating contributions are avoided and the spectrum is approximated by a rational function. It seems plausible that this approach works well at least in hyperbolic systems which admit a corresponding spectral structure [50,51].

To avoid the $\delta$ singularity of the spectrum at $\omega = 0$ let us start with the considerations from the correlation function

$$\tilde{C}_q(k) := C_q(k) - \langle u \rangle^2(q) \tag{20}$$

which decays to zero under some mixing assumption. In terms of this quantity the spectrum can be written as (cf equation (8))

$$I_q(\omega) = -\tilde{C}_q(0) + J_q(\mathrm{e}^{\mathrm{i}\omega}) + J_q(\mathrm{e}^{-\mathrm{i}\omega}) \qquad J_q(z) = \left( \tilde{\chi} \frac{z}{z\tilde{\chi} - \tilde{\omega} - \tilde{\gamma}(z)} \tilde{\chi} \right)_{11} \tag{21}$$

*using the abbreviations*

$$\tilde{\chi} = \begin{pmatrix} \tilde{C}_q(0) & \dots & \tilde{C}_q(M-1) \\ \vdots & & \vdots \\ \tilde{C}_q(M-1) & \dots & \tilde{C}_q(2M-2) \end{pmatrix} \qquad \tilde{\omega} = \begin{pmatrix} \tilde{C}_q(1) & \dots & \tilde{C}_q(M) \\ \vdots & & \vdots \\ \tilde{C}_q(M) & \dots & \tilde{C}_q(2M-1) \end{pmatrix}. \tag{22}$$

Again, the memory matrix $\tilde{\gamma}(z)$ has only one non-vanishing matrix element in the lower-right corner. From the discussion in the preceding section it is obvious that the expression (21) can be cast into the form of a continued fraction of order $M$ if the memory matrix is neglected. We also know that this expression may contain spurious poles if the order $M$ is chosen too large. As a consequence, the poles of the original spectrum can be obtained from the expression (21) only if the procedure described in section 2 is applied. On the other hand, the actual shape of the spectrum seems not to be modified by the spurious solutions in the general case, because these poles are typically at a large distance from the unit circle on which the expression (21) is evaluated.

† As mentioned in the introduction, a large temporally coarse graining $n \gg \ln N$ will lead to the ordinary statistical average $I_{q=0}(\omega)$.

As typical examples, we again treat data sets which have been obtained from the Lozi and Henon maps, respectively (cf equation (18)). To be consistent with the previous discussion let us again choose the local expansion rate as the observable $u(x)$. The principal features do not depend on this choice. Taking a time series that means an ensemble of size $N$, the correlation function (4) and the expectation value (3) have been computed directly for several $q$ values. Thereafter the data have been converted to the power spectrum with the help of (21) and (22) by neglecting the memory matrix.

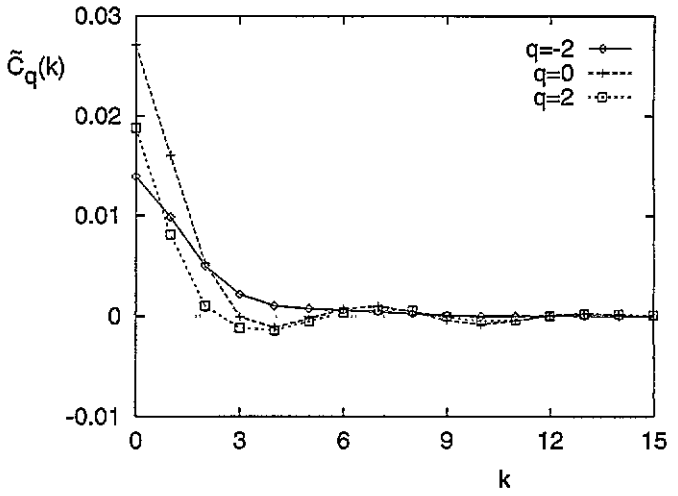


**Figure 2.** Correlation function of the Lozi map ($a = 1.7$, $b = 0.5$) obtained from an ensemble of size $N = 1.1 \times 10^7$ and $n = 30$.

Figure 2 shows typical results for the correlation function of the Lozi map. Due to its hyperbolic structure the correlations decay exponentially in the whole $q$ region. The power spectra obtained via the above-mentioned approach (cf figure 3) converge rapidly even for moderate orders of the expansion. This property has to be compared with the direct evaluation of expression (4), which is also displayed. The latter shows a noisy behaviour which shadows the actual form of the spectrum. For positive $q$ values a maximum in the spectrum and an oscillatory decay of the correlation function can be observed, respectively. It is so weak that it cannot be attributed to some definite periodic orbit of the dynamical system. The nearly Lorentzian shape for negative $q$ values relies on some symmetry property of the chosen observable. We will come back to this effect in the next section. The method converges well in the case of hyperbolic systems and allows for an accurate computation of power spectra.

The same procedure has been applied to the Henon map, especially in the vicinity of the phase-transition point. Figure 4 summarizes some results on the correlation function. It decays almost exponentially in the hyperbolic phase. Approaching the phase-transition point, a slowing down can be observed. It should be mentioned, however, that the statistical ensemble of size $N$ contains only a few members which represent the non-hyperbolic phase†. As a consequence, the statistical errors grow and the correlation function becomes noisy if the phase-transition point is approached. In particular, the data do not allow one to decide whether the correlation function decays in the non-hyperbolic phase. The power spectra obtained from (21) have been displayed in figure 5. The method converges well

† This property is the reason for the behaviour which has already been discussed in the introduction (cf figure 1).

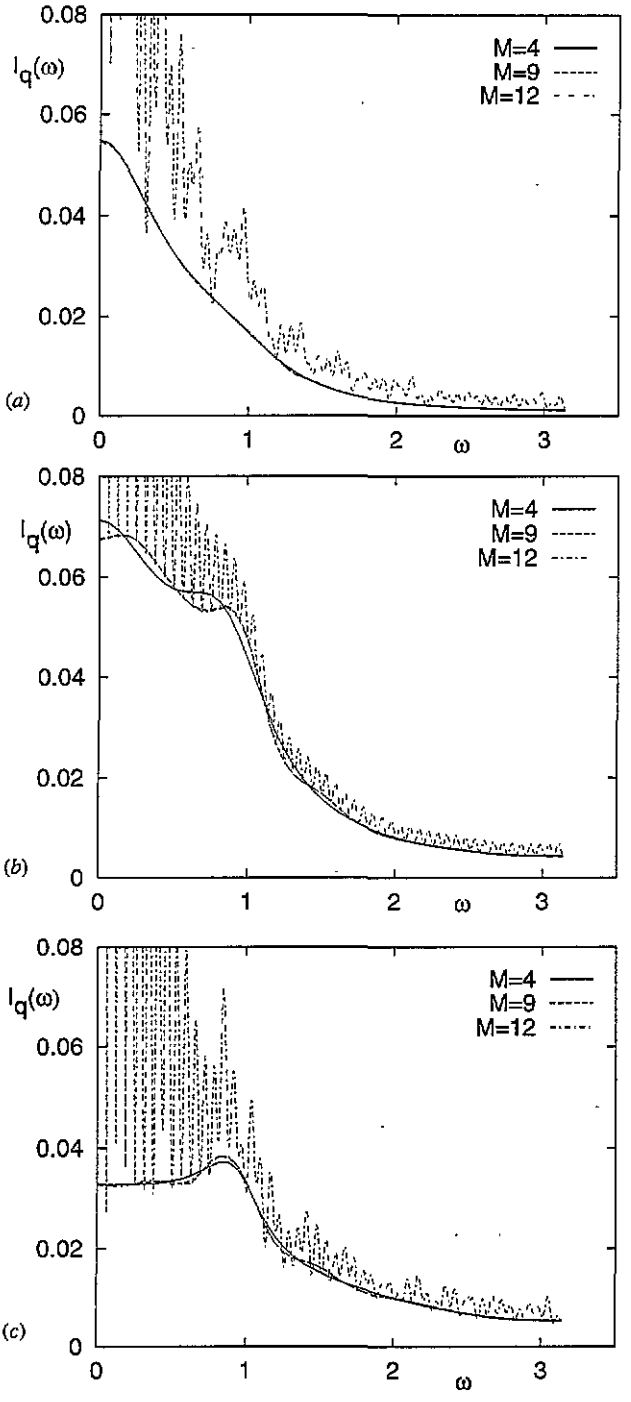


**Figure 3.** Power spectrum of the Lozi map obtained via a continued-fraction expansion of order $M$ for several $q$ values, (*a*) $q = -2$, (*b*) $q = 0$, (*c*) $q = 2$. The chain curve shows the direct calculation using (4) ($N = 5 \times 10^5$, $n = 100$). In all cases the expansions of order $M = 9$ and $M = 12$ coincide up to the line thickness.

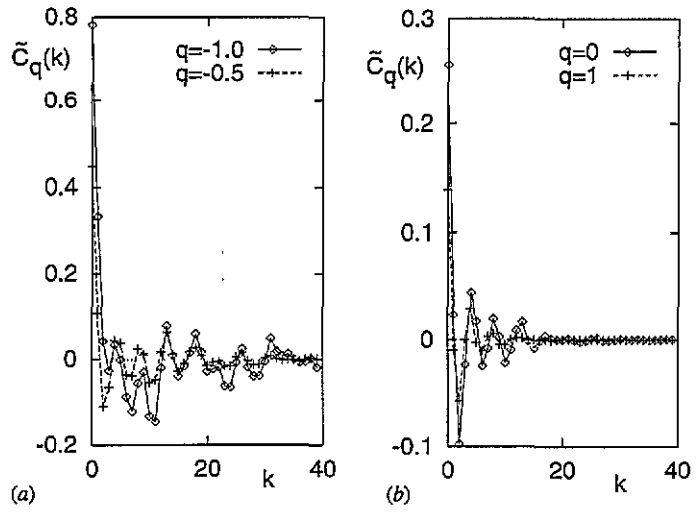


**Figure 4.** Correlation function of the Henon map ($a = 1.4$, $b = 0.3$) obtained from an ensemble of size $N \approx 9.8 \times 10^7$ and $n = 40$.

in the hyperbolic phase, indicating that the spectrum of the transfer operator consists of only a few relevant eigenvalues. Approaching the phase-transition point, the order of the expansion has to be increased to achieve convergence. This property is consistent with the assumption mentioned in the preceding section that the transition is caused by a continuous part of the spectrum. The spectrum, however, develops several sharp peaks, indicating the importance of periodic orbits of period 13 for the non-hyperbolic phase [52]. But near the phase-transition point $q = -1$, and especially in the non-hyperbolic phase, the method fails to produce reasonable quantitative results because of the above-mentioned noisy behaviour of the correlation functions.

As could be expected, the approach works well in hyperbolic situations which can be described approximately by a transfer operator with a discrete spectrum and few relevant eigenvalues. But also in non-hyperbolic cases, especially in intermittent situations, the main qualitative features are reproduced.

## 4. Periodic-orbit expansion

Although an expansion of statistical quantities in terms of periodic orbits may be difficult to apply to experimental data sets, because the extraction of sufficiently many periodic cycles of a certain length requires huge data sets, it is a convenient method to investigate the properties of model systems by means of a theoretical approach. It is the objective of this section to supplement the results of the previous sections and to shed some more light on the interpretation of the correlation functions and power spectra. As there is a lot of literature on this topic (e.g. [53, 54]) the method is only briefly outlined.

The main quantity of interest is a so-called zeta function (see appendix B for a derivation)

$$\frac{1}{\zeta_S(z)} = \exp\left[-\sum_{n=1}^{\infty}\frac{z^n}{n}\left(\sum_{p,n_p|n} n_p r_n(x_p)\right)\right]$$
$$r_n(x) := \frac{1}{|\det(1 - DT^n(x))|}\exp(qnU_n(x))\,. \tag{23}$$

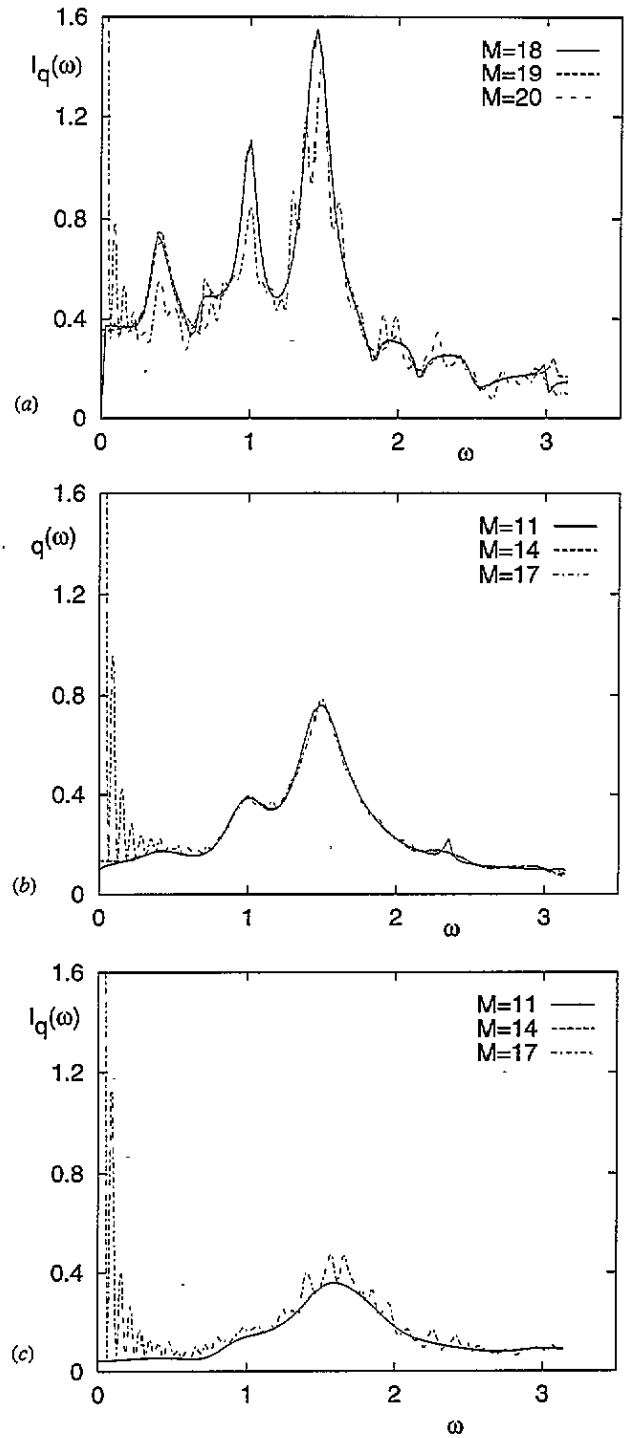


**Figure 5.** Power spectrum of the Henon map obtained via a continued-fraction expansion of order $M$ for several $q$ values, (*a*) $q = -0.5$, (*b*) $q = 0$, (*c*) $q = 1$. The chain curve shows the direct calculation using (4) ($N = 10^5$, $n = 100$).

Here $\sum_{p,n_p|n}$ denotes the summation over all prime cycles whose period divides $n$ and $x_p$ stands for an arbitrary phase-space point contained in this cycle. Its zeros $z^{(\nu)}$, $z^{(0)} < |z^{(1)}| \leqslant |z^{(2)}| \leqslant \cdots$ give the inverse eigenvalues of the transfer operator (6) and determine the pressure and the resonances of the power spectrum (4) via the relations (cf [28])

$$\Phi(q) = -\ln z^{(0)} \qquad \gamma_q^{(\nu)} + \mathrm{i}\omega_q^{(\nu)} = \frac{z^{(0)}}{z^{(\nu)}}. \tag{24}$$

Instead of using a Ruelle-type zeta function, which is known to be analytic in a bounded domain in $z$ for hyperbolic systems† [20] I use here a Selberg-type product [54] which is an entire function under the same conditions. This analytic property allows for a Taylor-series expansion of the quantity (23). From a finite truncation—that means from a polynomial—the zeros and hence the pressure and the first resonances can be determined accurately [56]. The fact that only short prime cycles enter this expansion, as well as its good convergence properties, at least in the hyperbolic case, make the quantity useful for theoretical investigations‡.

Furthermore, phase-space averages with respect to equilibrium measures $\mu_q$ of 'arbitrary' observables $f(x)$ can be obtained from expression (23) by taking a formal derivative (appendix B)

$$\int f(x)\,\mathrm{d}\mu_q \frac{1}{\zeta_S(z)} \sum_{n=1}^{\infty} z^n \left[ \sum_{p,n_p|n} n_p r_n(x_p) \right]$$

$$= \frac{1}{\zeta_S(z)} \sum_{n=1}^{\infty} z^n \left[ \sum_{p,n_p|n} n_p \left( \frac{1}{n} \sum_{k=0}^{n-1} f\left(T^k(x_p)\right) \right) r_n(x_p) \right] \qquad z \to z^{(0)}. \tag{25}$$

Equation (25) has to be evaluated at the smallest zero of the zeta function. But, as the last factors on both sides contain a pole which is cancelled by the zeta function, the limit $z \to z^{(0)}$ has to be considered. The second reason for keeping the common factors on both sides is not to destroy the analytic structure of the expression. As (25) is obtained directly from the derivative of an entire function, both sides admit a Taylor-series representation. Hence (25) can again be evaluated by expanding both sides in powers of $z$ and it has good convergence properties§. By choosing $f(x) = u(T^k(x))u(x)$, an expansion of the full correlation function (4) in terms of periodic orbits is obtained. Inspecting the right-hand side of (25), this expression is mainly determined by the diverse prime-cycle correlation functions.

Periodic orbits for the Lozi and the Henon map can be obtained easily. For reference with related work, table 3 contains the number of prime cycles that have been obtained up to period 18 and 19, respectively. By evaluating expression (25), the topological pressure, its derivative and the correlation function are computed from the prime-cycle data. Typical results for the correlation function are summarized in figures 6 and 7. As long as the argument of the correlation function does not exceed the order of the prime-cycle expansion, i.e. for the maximal period of the incorporated prime cycle, a reasonable convergence is observed for the hyperbolic Lozi map in the whole $q$ region. But it should be mentioned that the correlation function obtained from the expansion is nearly periodic with the order of the

† For the special case of a topological zeta function the meromorphic property can be proven [55].

‡ I do not intend to go into the details of the evaluation. It should be stressed, however, that the expansion can be considerably improved by using information about the symbolic dynamics or the symmetries of the system [53, 57].

§ As the observable $f(x)$ is rather arbitrary, one has obtained a representation of equilibrium measures in terms of periodic orbits which, to the authors best knowledge, cannot be found in the literature.

**Table 3.** Number of prime cycles, dependening on their period $n_p$, for the Lozi map ($a = 1.7$, $b = 0.5$) and the Henon map ($a = 1.4$, $b = 0.3$).

| $n_p$ | 1 | 2 | 3 | 4 | 5 | 6 | 7 | 8 | 9 | 10 |
|---|---|---|---|---|---|---|---|---|---|---|
| Lz | 1 | 1 | 0 | 1 | 0 | 4 | 4 | 7 | 10 | 12 |
| Hn | 1 | 1 | 0 | 1 | 0 | 2 | 4 | 7 | 6 | 10 |
| $n_p$ | 11 | 12 | 13 | 14 | 15 | 16 | 17 | 18 | 19 | |
| Lz | 18 | 32 | 56 | 78 | 122 | 180 | 282 | 439 | — | |
| Hn | 14 | 19 | 32 | 44 | 72 | 102 | 165 | 228 | 346 | |

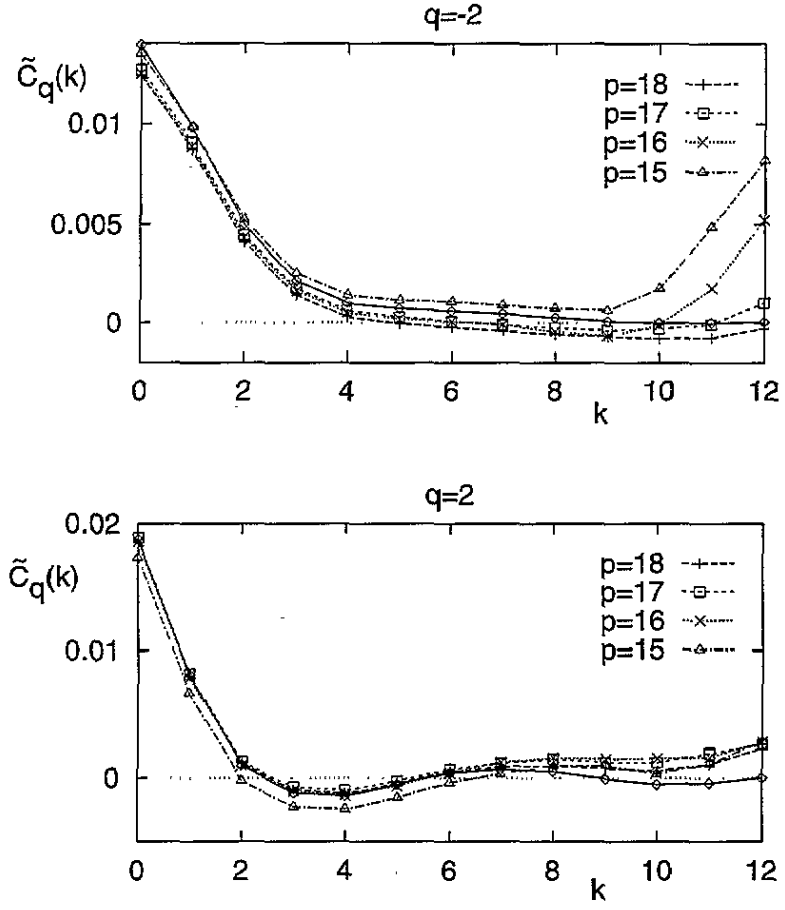


**Figure 6.** Correlation function of the Lozi map obtained from a prime-cycle expansion of order $p$. For comparison the result of the direct calculation (cf figure 2) is shown as a full curve.

expansion. Inspecting the expression (25), this observation is not surprising as the prime-cycle expansion approximates the equilibrium measure by $\delta$ peaks with appropriate weights. For the Henon map the results are similar in the hyperbolic phase (cf figure 7). But as one approaches the phase-transition point the expansion fails to converge sufficiently rapidly. Only qualitative features are reproduced, particularly the apparent degree of periodicity of the correlation function.

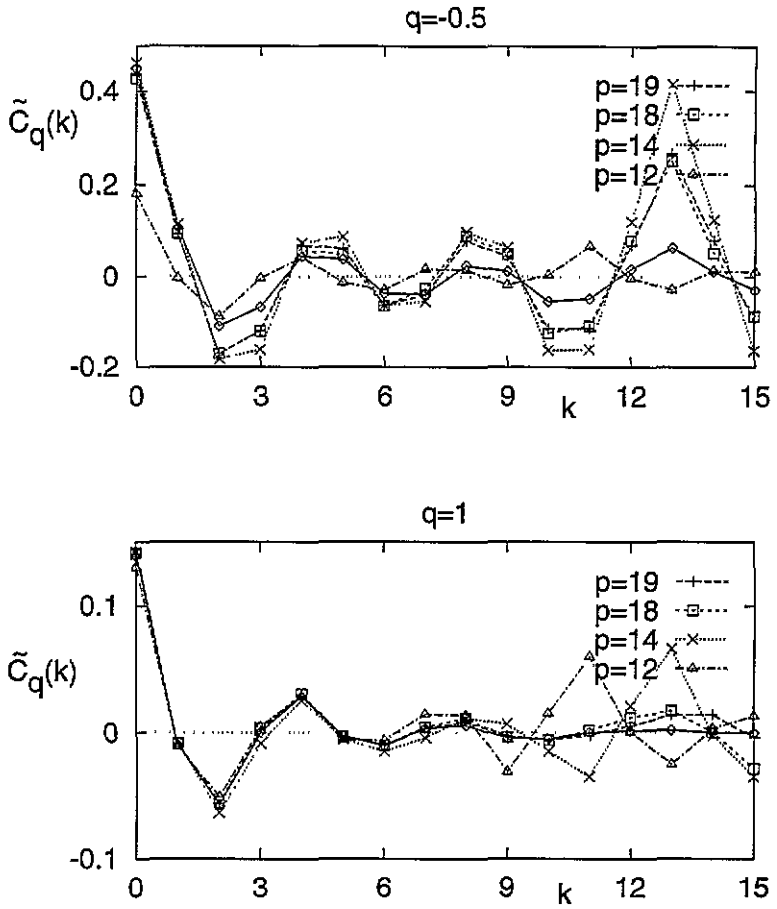


**Figure 7.** Correlation function of the Henon map obtained from a prime-cycle expansion of order $p$. For comparison, the result of the direct calculation (cf figure 4) is shown as a full cuve.

The results are to be supplemented with an analysis of the spectrum of the transfer operator using the zeta function (23). Approximate expressions for the largest eigenvalues can be obtained via the zeros of a truncated Taylor-series expansion of (23). Figures 8 and 9 show the results obtained in this way for two adjacent orders of the expansion. The zero with the lowest absolute value which determines the pressure shows the best convergence. The convergence properties decrease if one considers larger values.

In the case of the Lozi map (cf figure 8) the high-$q$ region is characterized by eigenvalues reflecting roughly a period-8 behaviour. This part of the spectrum comes from highly unstable prime cycles of period 7 and 8 which are favoured by the large $q$ values. The direct computation of the correlation functions (cf figures 2 and 6) reflects this fact too. The spectrum in the low-$q$ region is mainly determined by a negative eigenvalue with absolute value slightly smaller than the largest one. This behaviour is induced by a weakly unstable period-2 prime cycle. The correlation function does not show the corresponding oscillating behaviour as the observable, i.e. the local expansion rate $\lambda(x)$ is not 2-periodic on this orbit. It takes the same value on both phase-space points. Due to this symmetry property the decay of the correlation function is governed by prime cycles of higher periodicity.

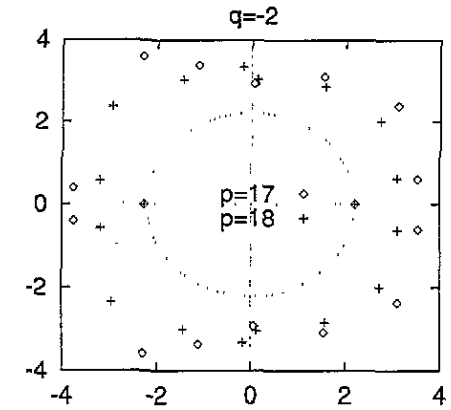


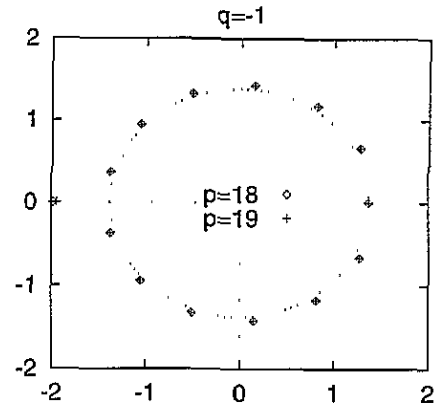


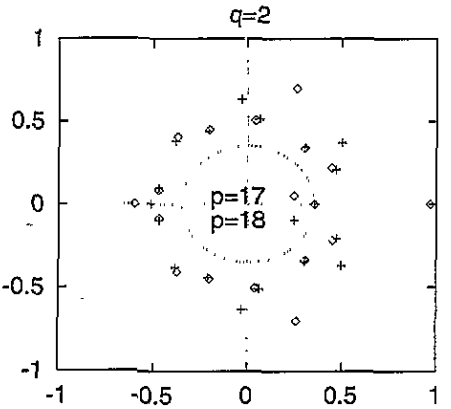


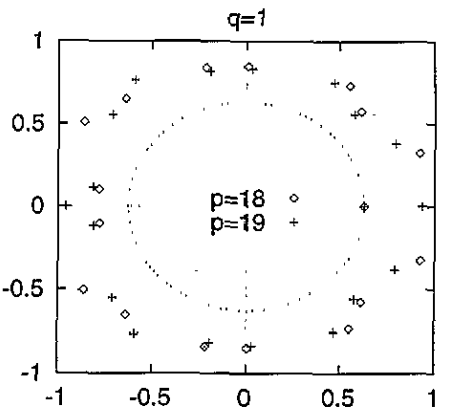


**Figure 8.** Zeros of the zeta function for two orders $p$ of the polynomial truncation for the Lozi map ($a = 1.7$, $b = 0.5$). The dotted circle indicates the absolute value of the smallest zero.

**Figure 9.** Zeros of the zeta function for two orders $p$ of the polynomial truncation for the Henon map ($a = 1.4$, $b = 0.3$) in the hyperbolic ($q = -1$) and non-hyperbolic ($q = 1$) phase. The dotted circle indicates the absolute value of the smallest zero.

The properties of the Henon map in the hyperbolic phase are comparable to those of the Lozi map (cf figure 9). But, as the phase-transition point is approached, the smallest zero becomes degenerate with a circle of zeros emerging from a nearly stable period-13 prime cycle which is known to mainly determine the phase transition. The corresponding features are clearly seen in the correlation function (cf figures 3 and 7). Due to this mechanism, the enhancement of the correlations in the non-hyperbolic phase can be understood. It remains, however, an open question whether the correlation function in this phase decays. A persistent oscillating part would indicate a loss of ergodicity and a decomposition of the equilibrium measure into different ergodic components. Such a behaviour typically occurs at phase transition points [20]. It would be interesting to detect these components in the actual dynamical system.

In contrast to the direct expansion of the correlation function in terms of periodic orbits, which works only for finite-time arguments, the determination of the low-order resonances, which means the long-time behaviour, from the zeta function works quite well. On the other hand the method does not yield the residues and therefore the actual shape of the

correlation function. In this respect both approaches deal with different asymptotic cases and support the results obtained from the direct simulation.

## 5. Conclusion

Continued-fraction techniques are suitable for the calculation of thermodynamic quantities, at least if spurious solutions which arise out of approximately invariant subspaces of the transfer operator have been removed. The approach seems to converge well and estimates of the finitely truncated matrix representation of the transfer operator yield some qualitative features of its spectral structure. Although the evaluation of the pressure does not lead to a detailed description, some global properties like phase transitions can be detected. The computation of the corresponding power spectra may reveal a deeper insight into the local structure of the underlying dynamics. The remaining unsolved problem concerns the choice of the observable $u(x)$. From the practical point of view the local expansion rate is inaccessible. But investigations on model systems support the conjecture that the detailed structure of the observable does not influence qualitative properties. Only the presence of higher-order phase transitions or some special local features of the dynamics may depend on the chosen function [27, 31, 58]. Further work in this direction is necessary. Nevertheless, the application of the method for the evaluation of experimental data sets seems promising and is in progress.

## Acknowledgments

The author is indebted to the Deutsche Forschungsgemeinschaft for financial support by a scholarship. This work was performed within a program of the Sonderforschungsbereich 185 Darmstadt–Frankfurt, FRG.

## Appendix A.

The correlation function and the power spectrum (4) can be expressed in terms of the transfer operator (6) acting on a function space†. Its dual space is considered as a measure space with elements $\langle\nu|$ and $\langle\nu|h\rangle := \int h(x)\,\mathrm{d}\nu$. In terms of the eigenelements $|h_q^{(0)}\rangle$ and $\langle\nu_q^{(0)}|$ of the operator (6) corresponding to the largest (positive) eigenvalue $\lambda_q^{(0)}$, the quantities of interest read [22]

$$\tilde{C}_q(k) = \langle\nu_q^{(0)}|\,\delta_q u\,(\mathcal{H}_q^u/\lambda_q^{(0)})^k(\,\delta_q u\,h_q^{(0)})\rangle \qquad I_q(\omega) = -\tilde{C}_q(0) + J_q(\mathrm{e}^{\mathrm{i}\omega}) + J_q(\mathrm{e}^{-\mathrm{i}\omega})\,. \tag{A1}$$

Here the abbreviations $\delta_q u\,(x) := u(x) - \langle u\rangle(q)$ and

$$J_q(z) = \langle\nu_q^{(0)}|\,\delta_q u\,\frac{z}{z - \mathcal{H}_q^u/\lambda_q^{(0)}}\,\delta_q u\,h_q^{(0)}\rangle \tag{A2}$$

have been used. To derive the expression (21) a projection operator technique can be applied to (A2) (cf [38]). Starting from the 'observables' $|\tilde{g}_1\rangle := |\,\delta_q u\,h_q^{(0)}\rangle$ and $\langle\tilde{\nu}_1| := \langle\nu_q^{(0)}|\,\delta_q u$, define a set of functions and measures by the recursion relations

$$|\tilde{g}_{n+1}\rangle := \left(\frac{\mathcal{H}_q^u}{\lambda_q^{(0)}}\right)|\tilde{g}_n\rangle \qquad \langle\tilde{\nu}_{n+1}| := \langle\tilde{\nu}_n|\left(\frac{\mathcal{H}_q^u}{\lambda_q^{(0)}}\right) \qquad 1 \leqslant n \leqslant M-1\,. \tag{A3}$$

† The precise definition of the function space is a serious and in general unsolved problem. In the simple case of piecewise analytic expanding maps the space consists of piecewise analytic functions.

With these sets a projection operator

$$\mathcal{P} = \sum_{kl} |\tilde{g}_k\rangle(\tilde{\chi}^{-1})_{kl}\langle\tilde{\nu}_l|$$

$$\tilde{\chi}_{kl} = \langle\tilde{\nu}_k|\tilde{g}_l\rangle = \langle\nu_q^{(0)}|\,\delta_q u\left(\frac{\mathcal{H}_q^u}{\lambda_q^{(0)}}\right)^{k+l-2}\delta_q u\, h_q^{(0)}\rangle = \tilde{C}_q(k+l-2) \tag{A4}$$

and its complement $\mathcal{Q} = 1 - \mathcal{P}$ can be constructed. Applying the well known operator identity [49]

$$\mathcal{P}\frac{1}{z-\mathcal{L}}\mathcal{P} = \mathcal{P}\left[z - \mathcal{P}\mathcal{L}\mathcal{P} - \mathcal{P}\mathcal{L}\mathcal{Q}\frac{1}{z-\mathcal{Q}\mathcal{L}\mathcal{Q}}\mathcal{Q}\mathcal{L}\mathcal{P}\right]^{-1}\mathcal{P} \tag{A5}$$

to the expression (A2) we obtain immediately (21) with

$$\tilde{\omega}_{kl} = \langle\tilde{\nu}_k|\left(\frac{\mathcal{H}_q^u}{\lambda_q^{(0)}}\right)\tilde{g}_l\rangle = \langle\nu_q^{(0)}|\,\delta_q u\left(\frac{\mathcal{H}_q^u}{\lambda_q^{(0)}}\right)^{k+l-1}\delta_q u\, h_q^{(0)}\rangle = \tilde{C}_q(k+l-1)$$
$$\tilde{\gamma}_{NN}(z) = \langle\nu_q^{(0)}|\,\delta_q u\,\mathcal{H}_q^u\mathcal{Q}\frac{1}{z\lambda_q^{(0)} - \mathcal{Q}\mathcal{H}_q^u\mathcal{Q}}\mathcal{Q}\mathcal{H}_q^u h_q^{(0)}\rangle/\lambda_q^{(0)}\,. \tag{A6}$$

If the transfer operator admits an $M_0$-dimensional invariant subspace which contains the function $\delta_q u\,(x)h_q^{(0)}(x) = \tilde{g}_1(x)$ then $\mathcal{Q}\mathcal{H}_q^u\tilde{g}_{M_0} = 0$ holds. Choosing $M = M_0$, the expression (21) becomes exact with $\tilde{\gamma}(z) = 0$. As the observables $\tilde{g}_1$ and $\tilde{\nu}_1$ have vanishing expectation value, $\langle\nu_q^{(0)}|\tilde{g}_1\rangle = 0$, $\langle\tilde{\nu}_1|h_q^{(0)}\rangle = 0$, the correlation function (20) decays and the $\delta$ peak of the power spectrum at $\omega = 0$ is suppressed. Otherwise this singularity would influence a finite-pole approximation.

## Appendix B.

Consider the transfer operator

$$(\mathcal{H}_{q,\epsilon}^u h)(x) = \int \delta(x - T(y))\,\mathrm{e}^{qu(y)+\epsilon f(y)}h(y)\,\mathrm{d}y\,. \tag{B1}$$

In the case $\epsilon = 0$ its eigenvalues coincide with those of expression (6), whereas the derivative of the logarithm of the largest eigenvalue with respect to $\epsilon$ yields the expectation value (3) [20]. To analyse the spectrum of (B1) the zeta function

$$\frac{1}{\zeta_{S,\epsilon}(z)} := \det(1 - z\mathcal{H}_{q,\epsilon}^u) \tag{B2}$$

is a useful tool. Using the standard relations [53]

$$\det(1-\mathcal{L}) = \exp\left(-\sum_{n=1}^{\infty}\mathrm{Tr}(\mathcal{L}^n)\right)$$
$$\mathrm{Tr}((\mathcal{H}_{q,\epsilon}^u)^n) = \sum_{x_\alpha\in\mathrm{Fix}(T^n)}\frac{1}{|\det(1-DT^n(x_\alpha))|}\exp\left(\sum_{k=0}^{n-1}[qu(T^k(x_\alpha)) + \epsilon f(T^k(x_\alpha))]\right) \tag{B3}$$

the zeta function (B2) can be cast into the form

$$\frac{1}{\zeta_{S,\epsilon}(z)} = \exp\left(-\sum_{n=1}^{\infty}z^n\left[\sum_{x_\alpha\in\mathrm{Fix}(T^n)}\frac{1}{|\det(1-DT^n(x_\alpha))|}\right.\right. \tag{B4}$$
$$\left.\left.\times\ \exp\left(\sum_{k=0}^{n-1}[qu(T^k(x_\alpha)) + \epsilon f(T^k(x_\alpha))]\right)\right]\right)\,. \tag{B5}$$

Changing the summation over all fixed points of $T^n$ to a summation over all prime cycles in a standard way [53] the equation determining the zeros of the zeta function and its derivative with respect to $\epsilon$ at $\epsilon = 0$ finally yields expressions (23) and (25) by taking the relation

$$-\frac{\mathrm{d}\ln(z^{(0)})}{\mathrm{d}\epsilon}\bigg|_{\epsilon=0} = \int f(x)\,\mathrm{d}\mu_q \tag{B6}$$

into account.

## References


[1] Halsey T C, Jensen M H, Kadanoff L P, Procaccia I and Shraiman B I 1986 *Phys. Rev.* A **33** 1141
[2] Glazier J A, Jensen M H, Libchaber A and Stavans J 1986 *Phys. Rev.* A **34** 1621
[3] Gwinn E G and Westervelt R M 1987 *Phys. Rev. Lett.* **59** 157
[4] Cumming A and Linsay P S 1987 *Phys. Rev. Lett.* **59** 1633
[5] Glazier J A, Gunaratne G and Libchaber A 1988 *Phys. Rev.* A **37** 523
[6] Mino M, Yamazaki H and Nakamura K 1989 *Phys. Rev.* B **40** 5279
[7] Yamazaki H and Mino M 1989 *Prog. Theor. Phys. Suppl.* **98** 400
[8] Yazaki T, Sugioka S, Mizutani F and Mamada H 1990 *Phys. Rev. Lett.* **64** 2515
[9] Barkley D and Cumming A 1990 *Phys. Rev. Lett.* **64** 327
[10] Casdagli M, Eubank S, Farmer J D and Gibson J 1991 *Physica* **51D** 52
[11] Sinai Ya G 1972 *Usp. Math. Nauk.* **27** 21
[12] Ruelle D 1976 *Am. J. Math.* **98** 619
[13] Fujisaka H and Inoue M 1987 *Prog. Theor. Phys.* **77** 1334
[14] Paladin G and Vulpiani A 1987 *Phys. Rep.* **156** 147
[15] Grassberger P, Badii R and Politi A 1988 *J. Stat. Phys.* **51** 135
[16] Bessis D, Paladin G, Turchetti G and Vaienti S 1988 *J. Stat. Phys.* **51** 109
[17] Mori H, Hata H, Horita T and Kobayashi T 1989 *Prog. Theor. Phys. Suppl.* **99** 1
[18] Moser H R, Meier P F and Waldner F 1993 *Phys. Rev.* B **47** 217
[19] Bowen R 1975 *Equilibrium States and the Ergodic Theory of Anosov Diffeomorphisms (Lecture Notes in Mathematics 470)* (Berlin: Springer)
[20] Ruelle D 1978 *Thermodynamical Formalism (Encyclopedia of Mathematics and its Applications 5)* (Reading, MA: Addison-Wesley)
[21] Walters P 1982 *An Introduction to Ergodic Theory* (New York: Springer)
[22] Just W and Fujisaka H 1993 *Physica* **64D** 98
[23] Fujisaka H, Yamaguchi A and Inoue M 1989 *Prog. Theor. Phys.* **81** 1146
[24] Tomita K, Hata H, Horita T, Mori H, Morita T, Okamoto H and Tominaga H 1989 *Prog. Theor. Phys.* **81** 1124
[25] Feigenbaum M J, Procaccia I and Tel T 1989 *Phys. Rev.* A **39** 5359
[26] Wang X J 1989 *Phys. Rev.* A **40** 6647
[27] Just W 1990 *Phys. Lett.* **150A** 362
[28] Fujisaka H and Shibata H 1991 *Prog. Theor. Phys.* **85** 187
[29] Horita T, Hata H, Mori H, Morita T, Tomita K, Kuroki S and Okamoto H 1988 *Prog. Theor. Phys.* **80** 793
[30] Just W and Fujisaka H 1991 *Phys. Lett.* **158A** 385
[31] Just W and Fujisaka H 1992 *J. Phys. A: Math. Gen.* **25** 3567
[32] Shibata H, Fujisaka H and Mori H 1992 *Physica* **189A** 554
[33] Kobayashi T, Fujisaka H and Just W 1993 *Phys. Rev.* E **47** 3196
[34] Badii R, Finardi M, Broggi G and Sepulveda M A 1992 *Physica* **58D** 304
[35] Fukushima K and Yamada T 1993 Order-$q$ power spectrum of an intermittency observed in a coupled electronic circuit *Preprint*
[36] Fujisaka H and Yamada T 1993 A new approach to multiplicative stochastic process II—infinite number time correlations *Preprint*
[37] Fujisaka H and Inoue M 1987 *Prog. Theor. Phys.* **78** 1203
[38] Just W 1992 *J. Stat. Phys.* **67** 271
[39] Fujisaka H 1993 private communication
[40] Fujisaka H, Shigematsu H and Eckhardt B 1993 *Z. Phys.* B **92** 235
[41] Szepfalusy P and Tel T 1986 *Phys. Rev.* A **34** 2520
[42] Fujisaka H and Inoue M 1987 *Prog. Theor. Phys.* **78** 268

[43] Mori N, Kobayashi T, Hata H, Morita T, Horita T and Mori H 1989 *Prog. Theor. Phys.* **81** 60
[44] Jones W B and Thorn W J 1980 *Continued Fractions, Analytic Theory and Applications (Encyclopedia of Mathematics and its Application 11)* (Reading, MA: Addison-Wesley)
[45] Fujisaka H 1983 *Prog. Theor. Phys.* **70** 1264
[46] Hata H, Horita T, Mori H, Morita T and Tomita K 1988 *Prog. Theor. Phys.* **80** 809
[47] Eckhardt B and Yao D 1993 *Physica* **65D** 100
[48] Mori H 1965 *Prog. Theor. Phys.* **33** 423
[49] Fick E and Sauermann G 1990 *The Quantum Statistics of Dynamic Processes (Springer Series in Solid-State Sciences 86)* (Berlin: Springer)
[50] Ruelle D 1987 *J. Diff. Geom.* **25** 117
[51] Rugh H H 1992 *Nonlinearity* **5** 1237
[52] Artuso R, Aurell E and Cvitanovic P 1990 *Nonlinearity* **3** 361
[53] Artuso R, Aurell E and Cvitanovic P 1990 *Nonlinearity* **3** 325
[54] Eckhardt B 1991 Periodic orbit theory *Lecture Notes for the International School of Physics 'Enrico Fermi' on Quantum Chaos, Preprint*
[55] Shub M 1987 *Global Stability of Dynamical Systems* (New York: Springer)
[56] Christiansen F, Paladin G and Rugh H H 1990 *Phys. Rev. Lett.* **65** 2087
[57] Cvitanovic P and Eckhardt B 1992 Symmetry decomosition of chaotic dynamics *Preprint*
[58] Fujisaka H and Inoue M 1990 *Phys. Rev.* A **41** 5302